Article

Discovery Medicine 2025; 37(201): 2244–2255
https://doi.org/10.24976/Discov.Med.202537201.191

From Lipoxygenase to Lineage Fate: ALOX5 Drives Thyroid Cancer Progression via the Jagged1-Notch Axis–Mediated M2 Macrophage Polarization

Shangwei Li[1], Xiao Lin[2,*]

[1]Department of Breast and Thyroid Surgery, The People's Hospital of Cangnan, 325800 Wenzhou, Zhejiang, China
[2]Department of Breast and Thyroid Surgery, Rui'an People's Hospital, 325200 Wenzhou, Zhejiang, China
*Correspondence: 13968862673@163.com (Xiao Lin)
Submitted: 29 July 2025 Revised: 26 August 2025 Accepted: 2 September 2025 Published: 20 October 2025

Background: Arachidonate 5-lipoxygenase (ALOX5), a key enzyme in lipid metabolism and inflammation, has been linked to the progression of various cancer types. However, its specific function in thyroid cancer and the tumor immune microenvironment remains unclear.

Methods: ALOX5 expression in thyroid cancer tissues and cell lines was analyzed using The Cancer Genome Atlas (TCGA) and GTEx databases, quantitative reverse transcription polymerase chain reaction (RT-qPCR), and Western blotting. A series of cellular assays—namely cell counting kit-8 (CCK-8), 5-Ethynyl-2′-Deoxyuridine (EdU) incorporation, colony formation, wound closure, and Transwell invasion tests—were conducted to assess the impact of ALOX5 knockdown on cell proliferation, migration, and invasion. The expression levels of cytokines (C-C motif chemokine ligand 2 (CCL2) and colony-stimulating factor 1 (CSF1)) and M2 macrophage surface markers (Cluster of Differentiation 163 (CD163) and Cluster of Differentiation 206 (CD206)) were evaluated using RT-qPCR and Western blot analyses in both conditioned medium and co-culture models. Flow cytometry was performed to quantify the expression of CD163 and CD206 in THP-1–derived macrophages following exposure to conditioned medium from thyroid cancer cells or direct co-culture. Furthermore, expression levels of proteins associated with the Notch signaling pathway were evaluated, and rescue experiments with Jagged canonical Notch ligand 1 (Jagged1) overexpression were conducted to validate the specific role of this pathway.

Results: ALOX5 was significantly upregulated in thyroid cancer tissues and cell lines ($p < 0.001$). Silencing ALOX5 suppressed cell proliferation, migration, and invasion. Additionally, ALOX5 knockdown reduced CCL2 and CSF1 expression and inhibited M2 macrophage polarization. Mechanistically, ALOX5 positively regulated the Jagged1-Notch signaling pathway, as evidenced by decreased expression of Jagged1, Notch intracellular domain (NICD), Hairy/enhancer-of-split related with YRPW motif protein 1 (HEY1), and Hairy and enhancer of split-1 (HES1) upon ALOX5 silencing. Additionally, overexpression of Jagged1 reversed the inhibitory effects of ALOX5 knockdown on tumor cell behavior and the production of immunosuppressive cytokines.

Conclusion: ALOX5 promotes thyroid cancer progression and the polarization of immunosuppressive tumor-associated macrophage polarization through activation of the Jagged1-Notch signaling cascade. Inhibiting ALOX5 could represent a promising therapeutic avenue for managing thyroid cancer by concurrently restraining tumor progression and reshaping the immune landscape of the tumor microenvironment.

Keywords: ALOX5; thyroid cancer; tumor-associated macrophages; M2 polarization; Jagged1-Notch signaling pathway

Introduction

Thyroid cancer is the most commonly diagnosed endocrine malignancy, and its incidence has been steadily increasing in recent years, particularly among women [1,2]. While differentiated thyroid carcinomas, such as papillary thyroid carcinoma, generally have a favorable prognosis, a proportion of cases still experience challenges like tumor recurrence, aggressive invasion, and distant metastasis [3]. These clinical complexities highlight the urgent need to better elucidate the molecular mechanisms underlying thyroid cancer progression and to detect novel therapeutic targets for improving treatment outcomes.

Arachidonate 5-lipoxygenase (ALOX5), a key enzyme involved in arachidonic acid metabolic pathways, catalyzes the synthesis of leukotrienes—bioactive lipids that play a crucial role in immune modulation, inflammation, and oxidative stress [4]. Traditionally, ALOX5 has been associated with a spectrum of inflammatory conditions, such as asthma and atherosclerosis [5,6]. However, emerging evidence has underscored its pivotal role in cancer development. Investigations across multiple malignancies, including ovarian, bladder, and gastric cancers, have revealed that ALOX5 facilitates malignant cell growth, enhances invasive behavior, and promotes evasion of apoptosis [7–

9]. Furthermore, ALOX5 has been shown to modulate the tumor microenvironment, particularly by influencing immune cell infiltration and polarization [10,11]. Nevertheless, its expression profile, functional relevance, and underlying mechanisms in thyroid cancer remain largely unexplored.

The tumor immune microenvironment (TIME) is increasingly recognized as a key determinant of tumor progression and therapeutic resistance [12]. Within this complex cellular ecosystem, tumor-associated macrophages (TAMs) constitute a predominant and highly heterogeneous population of immune cells [13]. Due to their remarkable adaptability, TAMs are commonly classified into two major functional subtypes: M1 macrophages, which exhibit pro-inflammatory and anti-tumor properties, and M2 macrophages, which facilitate tumor growth by enhancing neovascularization, metastasis, and immune suppression [14,15]. It is well-documented that malignant cells secrete chemokines such as C-C motif chemokine ligand 2 (CCL2) and colony-stimulating factor 1 (CSF1), which recruit monocytes and drive their differentiation toward the M2-like phenotype [16]. However, the role of ALOX5 in regulating this signaling axis in thyroid cancer and its contribution to immune evasion remain to be elucidated.

Notch signaling represents a fundamental and evolutionarily conserved pathway that governs diverse cellular processes, including proliferation, differentiation, and immune responses [17]. In cancer, dysregulated Notch pathway activity has been linked to tumor progression, the induction of epithelial-to-mesenchymal transition (EMT), and profound remodeling of the tumor immune microenvironment [18,19]. Notably, the Notch ligand Jagged1 has been shown to induce M2 macrophage polarization, thereby promoting an immunosuppressive TME in several malignancies [20]. Although the involvement of ALOX5 in tumor progression and inflammation is widely recognized, its potential interaction with the Notch signaling pathway and its impact on macrophage polarization in thyroid cancer remain poorly understood, warranting further comprehensive investigation.

This study aimed to comprehensively elucidate the role of ALOX5 in thyroid tumorigenesis and immune modulation. Initially, this study assessed ALOX5 expression levels across thyroid cancer tissues and cultured cell models, followed by functional assays to determine its impact on critical tumor cell behaviors, including proliferation, migration, and invasion *in vitro*. Then, we examined the role of ALOX5 in regulating the expression of CCL2 and CSF1 and its influence on macrophage polarization toward the M2 phenotype. Finally, we explored the involvement of the Jagged1-Notch signaling pathway in mediating ALOX5-driven tumor progression and the immunosuppressive remodeling of the TIME. These findings provide novel insights into the oncogenic and immunomodulatory roles of ALOX5 in thyroid cancer and suggest the therapeutic potential of targeting the ALOX5-Jagged1-Notch axis.

Materials and Methods

Bioinformatics Analysis

ALOX5 expression in thyroid cancer and normal thyroid tissues was analyzed using the GEPIA 2 database (http://gepia2.cancer-pku.cn), which integrates RNA-seq data from The Cancer Genome Atlas (TCGA) and GTEx projects. Furthermore, expression levels of ALOX5 were compared between tumor and normal samples using the "Expression DIY" module, with statistical significance determined using a standard *t*-test.

Cell Culture

Human thyroid cancer cell lines (TPC-1, AW-CCH362; BCPAP, AW-CCH044; K1, AW-CCH573), the normal human thyroid follicular epithelial cell line (Nthy-ori 3-1, AW-CNH311), and the human monocytic cell line THP-1 (AW-CCH098) were obtained from Abiowell (Changsha, China). Cells were maintained in Roswell Park Memorial Institute 1640 (RPMI-1640) medium (11875093, Gibco, Shanghai, China) or Dulbecco's modified eagle medium (11965092, DMEM, Gibco, Shanghai, China) supplemented with 10% fetal bovine serum (A5670701, FBS, Gibco, Shanghai, China) and 1% penicillin-streptomycin (P1400, Solarbio, Beijing, China). All cultures were maintained in a humidified atmosphere at 37 °C with 5% CO_2. All cell lines were authenticated by short tandem repeat (STR) profiling and tested for mycoplasma contamination. All experimental protocols were performed under sterile conditions to avoid contamination.

Quantitative Reverse Transcription Polymerase Chain Reaction (RT-qPCR)

Total RNA was extracted using TRIzol reagent (I15596026CN, Invitrogen, CA, USA), following the manufacturer's instructions. cDNA was synthesized using a reverse transcription kit (RR037A, Takara, Otsu, Japan), and qPCR was performed using SYBR Green PCR Master Mix (4367659, Thermo Fisher Scientific, MA, USA). Gene expression levels were normalized to glyceraldehyde-3-phosphate dehydrogenase (GAPDH), and relative expression was determined using the $2^{-\Delta\Delta Ct}$ method. Primers used in qRT-PCR are listed below: *ALOX5*, Forward: 5′-GGAGAACCTGTTCATCAACCGC-3′; Reverse: 5′-CAGGTCTTCCTGCCAGTGATTC-3′. *CCL2*, Forward: 5′-AGAATCACCAGCAGCAAGTGTCC-3′; Reverse: 5′-TCCTGAACCCACTTCTGCTTGG-3′. *CSF1*, Forward: 5′-TGAGACACCTCTCCAGTTGCTG-3′; Reverse: 5′-GCAATCAGGCTTGGTCACCACA-3′. *CD206*, Forward: 5′-AGCCAACACCAGCTCCTCAAGA-3′; Reverse: 5′-CAAAACGCTCGCGCATTGTCCA-3′. Cluster of Differentiation 163 (*CD163*), Forward: 5′-

CCAGAAGGAACTTGTAGCCACAG-3′; Reverse: 5′-CAGGCACCAAGCGTTTTGAGCT-3′. *Jagged1*, Forward: 5′-TGCTACAACCGTGCCAGTGACT-3′; Reverse: 5′-TCAGGTGTGTCGTTGGAAGCCA-3′. Hairy/enhancer-of-split related with YRPW motif protein 1 (*HEY1*), Forward: 5′-TGTCTGAGCTGAGAAGGCTGGT-3′; Reverse: 5′-TTCAGGTGATCCACGGTCATCTG-3′. Hairy and enhancer of split-1 (*HES1*), Forward: 5′-GGAAATGACAGTGAAGCACCTCC-3′; Reverse: 5′-GAAGCGGGTCACCTCGTTCATG-3′. GAPDH, Forward: 5′-GTCTCCTCTGACTTCAACAGCG-3′; Reverse: 5′-ACCACCCTGTTGCTGTAGCCAA-3′.

Western Blotting

Cellular proteins were extracted using radioimmunoprecipitation assay (RIPA) lysis buffer (P0013B, Beyotime, Shanghai, China) containing protease and phosphatase inhibitors. The lysate was resolved by sodium dodecyl sulfate–polyacrylamide Gel Electrophoresis (SDS-PAGE) and then transferred onto polyvinylidene difluoride (PVDF) membranes. After blocking with 5% bovine serum albumin (ST2249, BSA, Beyotime, Shanghai, China), the membranes were incubated overnight at 4 °C with the following primary antibodies: ALOX5 (1:1000, ab169755, Abcam, Cambridge, UK), Jagged canonical Notch ligand 1 (Jagged1; 1:1000, ab109536, Abcam, Cambridge, UK), Notch intracellular domain (NICD; 1:1000, ab52627, Abcam, Cambridge, UK), HEY1 (1:500, ab154077, Abcam, Cambridge, UK), HES1 (1:1000, ab108937, Abcam, Cambridge, UK), CCL2 (1:2000, A7277, ABclonal, MA, USA), CSF1 (1:1000, A3019, ABclonal, MA, USA), and GAPDH (1:2500, ab9485, Abcam, Cambridge, UK). The next day, membranes were incubated for 1 hour at room temperature with species-specific horseradish peroxidase (HRP)-conjugated secondary antibodies (1:2000, ab205718, Abcam, Cambridge, UK). Protein signals were detected using an enhanced chemiluminescence (ECL), and band intensities were quantified using ImageJ software (version 5.0; Bio-Rad, Hercules, CA, USA). GAPDH served as the internal loading control, and the grayscale intensities of the target proteins were normalized to GAPDH for statistical analysis.

Cell Transfection

The *ALOX5* gene was knocked down using small interfering RNAs (siRNAs; si-ALOX5: GATTCACCATTGCAATCAA; RiboBio, Guangzhou, China), while Jagged1 overexpression was performed by transfecting cells with a pcDNA3.1-Jagged1 plasmid (Corues, Nanjing, China). The full-length coding sequence of Jagged1 used in this study is provided in the **Supplementary Material**. Transfections were conducted using Lipofectamine 3000 (L3000001, Invitrogen, CA, USA) following the manufacturer's protocol. Briefly, cells were seeded in 6-well plates at a density of 2×10^5 cells per well and incubated overnight until reaching 60–70% confluence. siRNA or plasmid DNA was diluted in medium, mixed with Lipofectamine 3000 reagent, and incubated for 15 minutes at room temperature before being added to the cells. After 6–8 hours, the transfection medium was replaced with complete growth medium. Finally, transfection efficiency was confirmed after 48 hours by RT-qPCR and Western blotting.

Cell Counting Kit-8 (CCK-8)

Cell viability was assessed using the cell counting kit-8 (CCK-8; CK04, Dojindo, Kumamoto, Japan). Transfected TPC-1 cells were seeded into 96-well plates at a density of 5×10^3 cells/well. After 24, 48, and 72 hours, 10 µL of CCK-8 reagent was added to each well and incubated for 2 hours. Finally, absorbance was measured at 450 nm using a microplate reader (ELX800, BioTek Instruments, VT, USA).

5-Ethynyl-2′-Deoxyuridine (EdU) Staining

Cell proliferation was further evaluated using an EdU staining kit (C0071, Beyotime, Shanghai, China). TPC-1 cells (3×10^4 per well) were seeded in 24-well plates and subsequently incubated with 10 µM EdU for 2 hours. The cells were then fixed with 4% paraformaldehyde, permeabilized, and processed following the kit protocol. Finally, images were captured using a fluorescence microscope, and the proportion of EdU-positive cells was determined to assess proliferation capacity.

Colony Formation Assay

Transfected cells (1000 per well) were seeded in 6-well plates and cultured for 14 days to allow colony formation. The colonies were then fixed with methanol and stained with 0.1% crystal violet. Finally, the images were captured for quantification. Colonies were quantified by counting the number of colonies formed, irrespective of their size.

Wound Healing Assay

TPC-1 cells were seeded in 6-well plates and cultured until reaching 90% confluence. A uniform scratch was made using a sterile pipette tip, and detached cells were gently removed by rinsing with PBS. The cells were then cultured in serum-free medium, and images of the wound area were captured at 0 and 24 hours. Migration rates were evaluated using ImageJ software.

Transwell Invasion Assay

Cell invasion was assessed using Transwell chambers coated with Matrigel. Briefly, 2×10^4 cells suspended in serum-free medium were loaded in the upper chamber, while medium containing 10% FBS, a chemoattractant, was added to the lower chamber. After 24 hours of incubation,

cells that invaded the lower surface of the membrane were fixed, stained with 0.1% crystal violet, and counted under a microscope.

Conditioned Medium (CM) Preparation and THP-1 Polarization Assay

To prepare CM, TPC-1 cells transfected with either si-NC or si-ALOX5 were cultured in serum-free medium for 48 hours. The collected supernatants were centrifuged to remove debris and then used to treat Phorbol 12-myristate 13-acetate (PMA)-differentiated THP-1 macrophages (100 ng/mL PMA, 24 hours), as previously described [21]. After 48 hours of CM exposure, the expression of M2 macrophage markers (Cluster of Differentiation 163 (CD163) and Cluster of Differentiation 206 (CD206)) was evaluated using flow cytometry and RT-qPCR.

Co-Culture of THP-1 Macrophages and TPC-1 Cells

THP-1–derived macrophages were co-cultured with TPC-1 cells in a Transwell system (0.4 µm pore size) to mimic the tumor immune microenvironment. Macrophages were seeded in the lower chamber, while tumor cells were seeded in the upper chamber, following a previously described method [22]. After 48 hours of co-culture, macrophages were collected to evaluate M2 polarization markers using flow cytometry and RT-qPCR. In parallel, PMA-differentiated THP-1 macrophages were stimulated with IL-4 (20 ng/mL) for 48 hours to induce M2 polarization, serving as a positive control.

Flow Cytometry

After treatment, macrophages were harvested, washed with PBS, and incubated with fluorochrome-conjugated antibodies against human CD163 (111803, BioLegend, CA, USA) and CD206 (321105, BioLegend, CA, USA) for 30 minutes at 4 °C in the dark. After staining, the cells were washed, resuspended in flow buffer (PBS containing 2% FBS), and analyzed using a BD FACSCantoTM II flow cytometer (BD Biosciences, CA, USA). Data were processed and analyzed using FlowJo software (version 10.0, BD Biosciences, CA, USA).

Statistical Analysis

Statistical analyses were performed using GraphPad Prism 9.0 (GraphPad Software, San Diego, CA, USA). All experiments were independently conducted at least three times. Data were presented as the mean ± standard deviation (SD). Comparisons between two groups were conducted using an unpaired Student's *t*-test, while comparisons among multiple groups were performed using one-way analysis of variance (ANOVA) followed by Tukey's post hoc test. A *p*-value of <0.05 was considered statistically significant.

Results

ALOX5 Exhibits Elevated Expression in Thyroid Cancer Samples and Cell Models

To evaluate ALOX5 expression in thyroid malignancies, we first analyzed publicly available datasets from TCGA and GTEx. The analysis showed a significant increase in *ALOX5* levels in thyroid cancer tissues compared

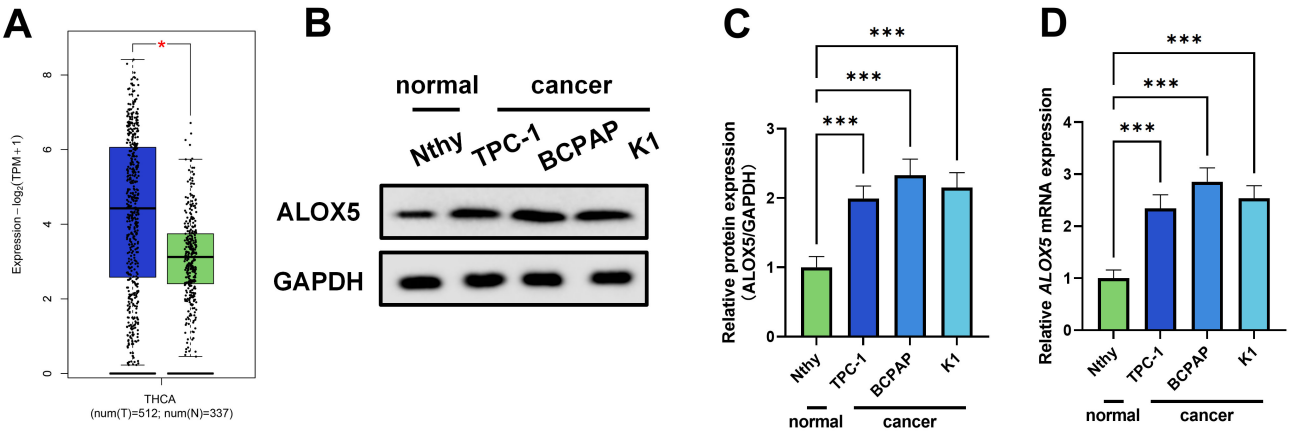

Fig. 1. Arachidonate 5-lipoxygenase (ALOX5) is substantially upregulated in thyroid cancer. (A) Differential expression of *ALOX5* in cancerous versus normal thyroid tissues based on TCGA and GTEx databases (analyzed using Student's *t*-test). (B) Representative Western blot analysis of ALOX5 protein expression in normal thyroid cells (Nthy) and thyroid cancer cell lines (TPC-1, BCPAP, K1). (C) Quantification of ALOX5 protein expression levels from three independent experiments (analyzed using ANOVA). (D) Quantitative reverse transcription polymerase chain reaction (RT-qPCR) analysis of *ALOX5* mRNA expression in normal thyroid cells (Nthy) and thyroid cancer cell lines (TPC-1, BCPAP, K1) (analyzed using ANOVA). All experiments were independently performed in triplicate. Data are presented as the mean ± SD. *$p < 0.05$, ***$p < 0.001$.

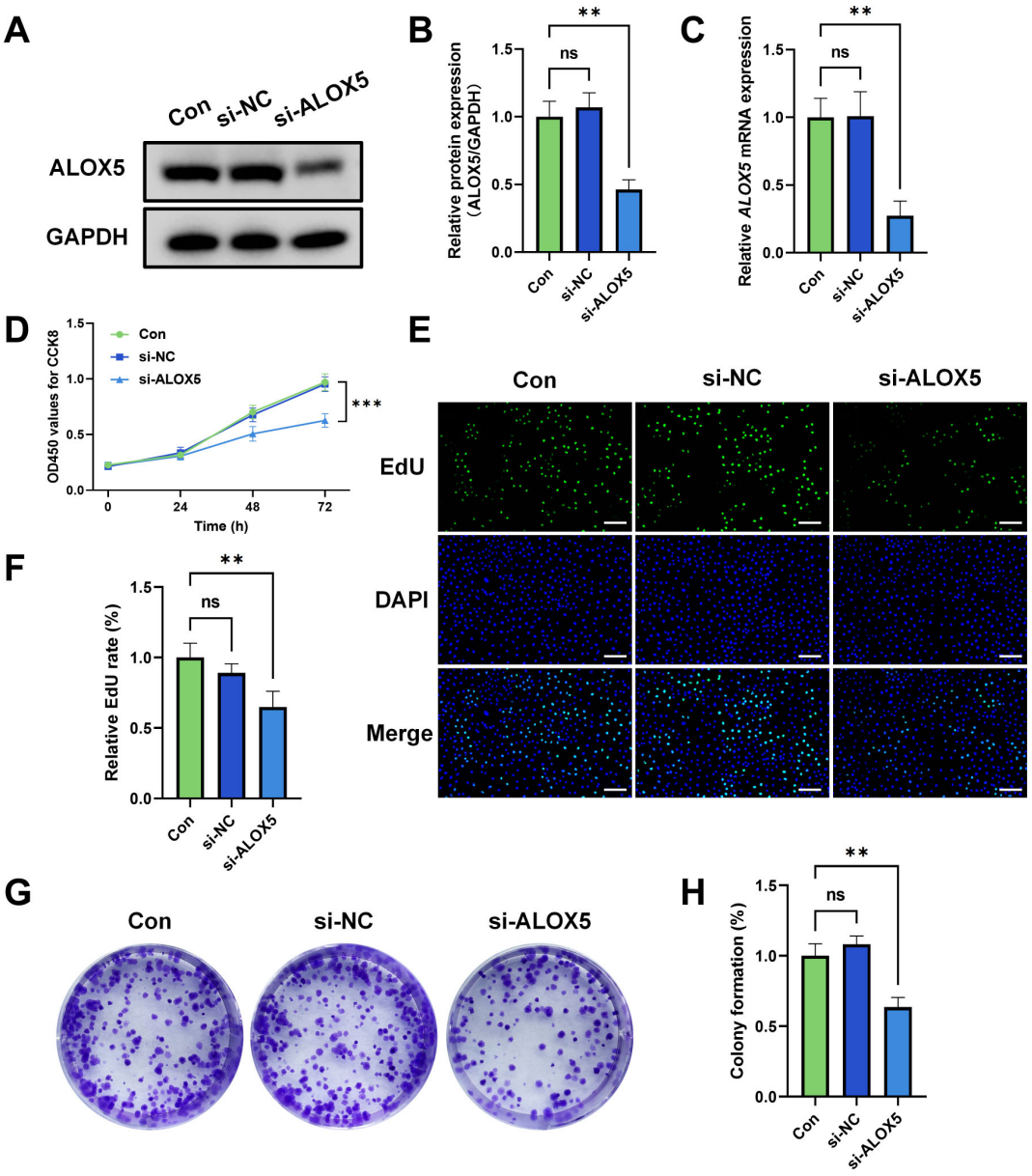

Fig. 2. Knockdown of ALOX5 inhibits the proliferation of thyroid cancer cells. (A) Representative Western blot analysis of ALOX5 protein levels in the control (con), negative control (si-NC), and ALOX5 knockdown (si-ALOX5) groups. (B) Quantification of ALOX5 protein expression levels from three independent experiments. (C) RT-qPCR analysis of *ALOX5* mRNA levels in the con, si-NC, and si-ALOX5 groups. (D) Cell proliferation of TPC-1 thyroid cancer cells in the three groups was assessed using the cell counting kit-8 (CCK-8), assay. (E) 5-Ethynyl-2′-Deoxyuridine (EdU) staining detected the proliferative capacity of TPC-1 cells (Scale bar: 50 µm). (F) Quantification of relative EdU-positive cell rate. (G) Colony formation assay evaluated the clonogenic ability of TPC-1 cells after 14 days of culture. (H) Quantification of colony formation. All experiments were independently repeated at least three times. Data are presented as the mean ± SD. Statistical significance for all panels was assessed using one-way ANOVA. ns $p > 0.05$, **$p < 0.01$, ***$p < 0.001$.

to non-tumorous thyroid counterparts (Fig. 1A, $p < 0.05$). Corroborating this observation, Western blotting revealed significantly higher ALOX5 protein levels in thyroid cancer cell lines (TPC-1, BCPAP, K1) compared to normal thyroid epithelial cells (Nthy; Fig. 1B,C, $p < 0.001$). Similarly, RT-qPCR analysis further confirmed a significant upregulation in *ALOX5* mRNA expression in thyroid cancer cells (Fig. 1D, $p < 0.001$), suggesting that ALOX5 may be involved in thyroid tumorigenesis.

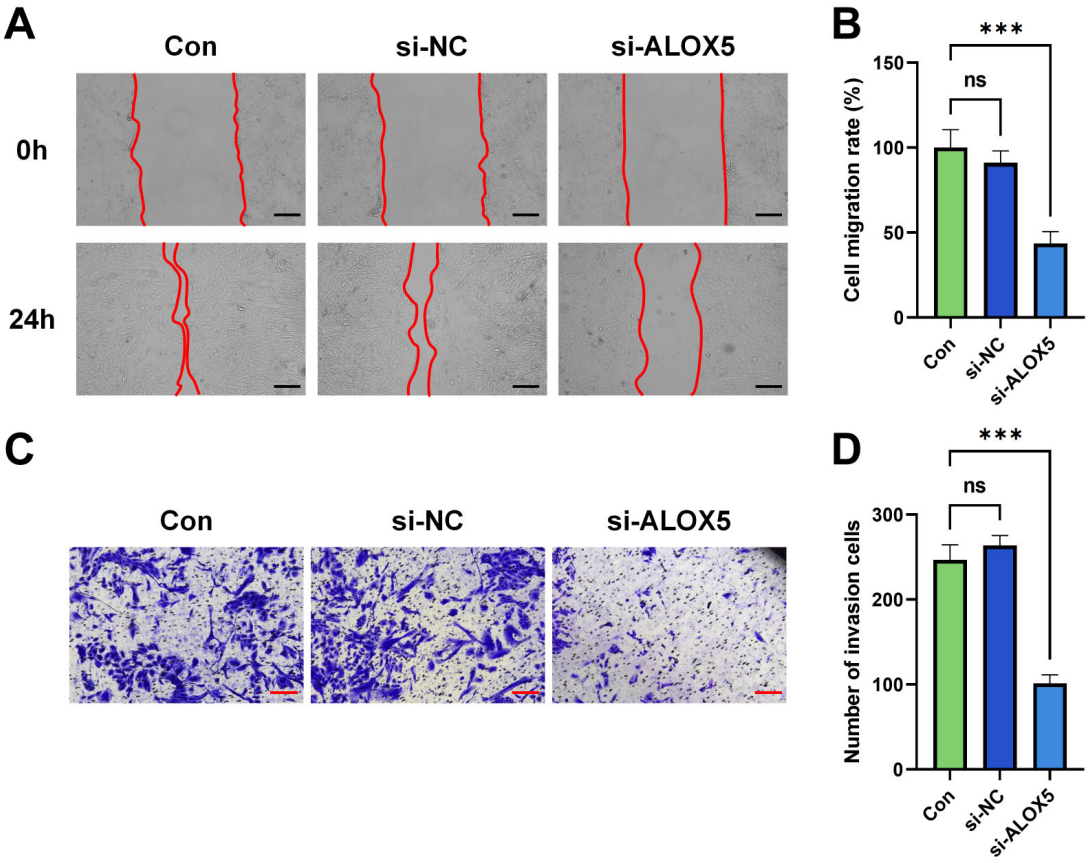

Fig. 3. Silencing ALOX5 compromises thyroid cancer cell motility and invasiveness. (A) Wound closure images following si-ALOX5 treatment in TPC-1 cells (Scale bar: 100 µm). (B) Quantitative assessment of the cell migration rate. (C) Transwell invasion assay illustrating reduced invasive capability post-ALOX5 knockdown (Scale bar: 100 µm). (D) Statistical analysis of the number of cells invading the membrane. All experiments were independently repeated at least three times. Data are presented as the mean ± SD. Statistical significance for all panels was assessed using one-way ANOVA. ns $p > 0.05$, ***$p < 0.001$.

Silencing ALOX5 Attenuates the Growth, Migration, and Invasiveness of Thyroid Cancer Cells

To elucidate the functional significance of ALOX5 in thyroid tumor biology, we conducted a series of *in vitro* assays following ALOX5 knockdown in TPC-1 cells. Knockdown efficiency was validated at both the protein and mRNA levels using Western blot and RT-qPCR analyses, respectively (Fig. 2A–C, $p < 0.01$). Functionally, ALOX5-deficient cells showed substantially reduced viability, as shown by the CCK-8 assay (Fig. 2D, $p < 0.001$), along with significantly suppressed DNA replication activity, as evidenced by EdU staining (Fig. 2E,F, $p < 0.001$).

Furthermore, colony formation assays demonstrated that ALOX5 silencing disrupted the long-term proliferative potential of TPC-1 cells (Fig. 2G,H, $p < 0.01$). Additionally, ALOX5 knockdown significantly impaired cell motility and invasive potential. Wound healing assays showed a reduced migratory capacity in si-ALOX5 cells (Fig. 3A,B, $p < 0.001$), while Transwell analysis demonstrated fewer cells penetrating the Matrigel-coated membrane, indicating diminished invasive capacity (Fig. 3C,D, $p < 0.001$). Collectively, these findings underscore of ALOX5 as in promoting thyroid cancer cell proliferation, migration, and invasion.

ALOX5 Regulates Cytokine Expression and Facilitates M2 Macrophage Polarization

To investigate the immunomodulatory role of ALOX5 within the tumor microenvironment, we first assessed its impact on cytokines involved in macrophage recruitment and polarization. Knockdown of ALOX5 in TPC-1 cells resulted in a significant decrease in both protein and mRNA levels of CCL2 and CSF1, as demonstrated by Western blot and RT-qPCR analyses (Fig. 4A–D, $p < 0.001$). To evaluate the functional consequence of these changes, CM from control or si-ALOX5–transfected TPC-1 cells was applied to THP-1–derived macrophages. Flow cytometry revealed a significant reduction in the expression of M2 surface markers CD163 and CD206 in the si-ALOX5 group (Fig. 4E–G, $p < 0.001$), which was further supported by RT-qPCR analysis of M2-associated gene expression (Fig. 4H, $p < 0.001$).

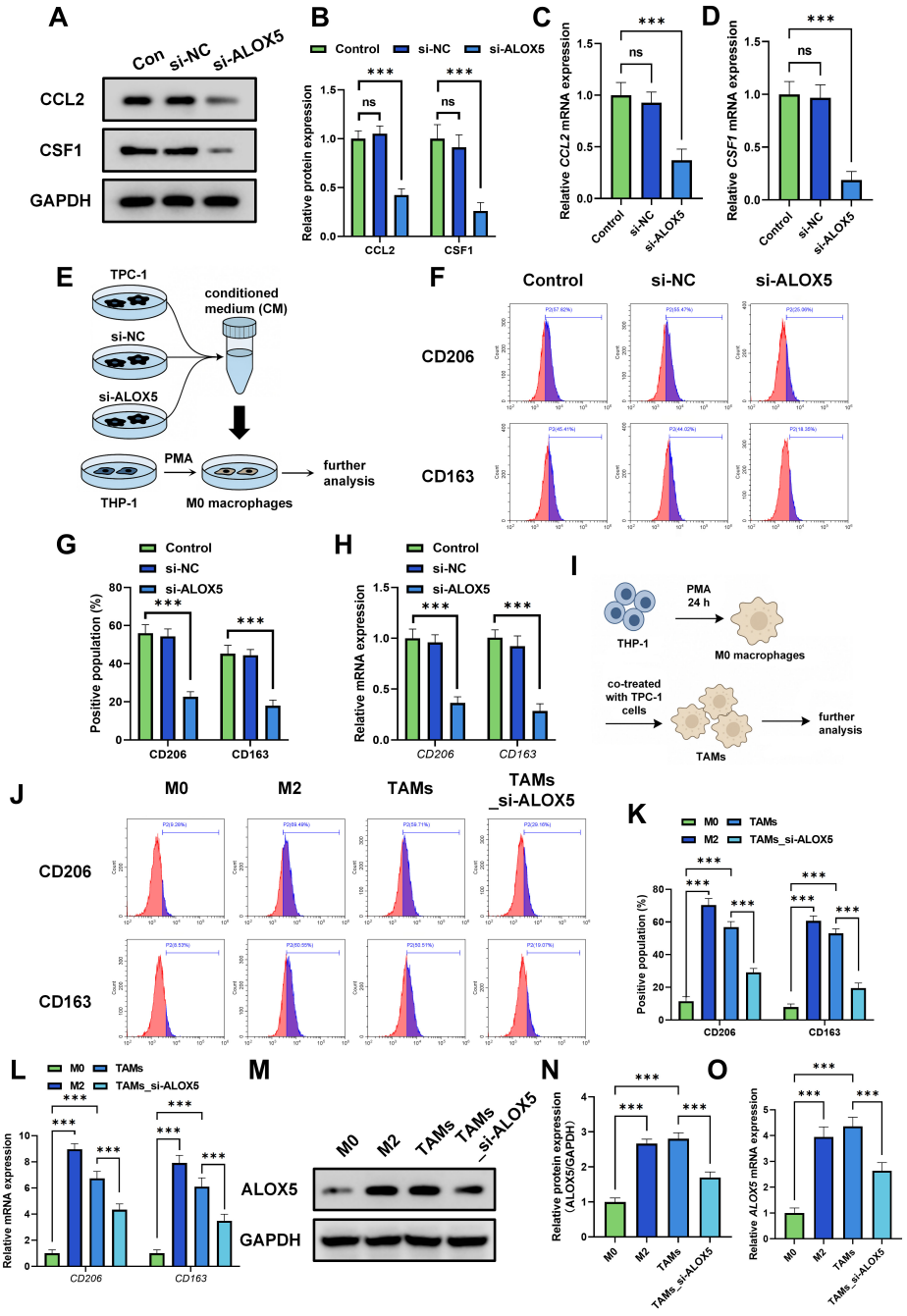

Fig. 4. ALOX5 knockdown reduces C-C motif chemokine ligand 2 (CCL2) and colony-stimulating factor 1 (CSF1) expression and inhibits M2 macrophage polarization. (A) Expression of CCL2 and CSF1 proteins in si-ALOX5–treated TPC-1 cells, assessed using Western blot analysis. Representative Western blot images are shown. (B) Quantification of CCL2 and CSF1 protein expression levels from three independent experiments. (C,D) RT-qPCR analysis of CCL2 and CSF1 mRNA levels. (E) Schematic illustration of the experimental protocol using CM to induce M2 polarization. (F,G) Flow cytometry was performed to analyze the expression of the M2 markers (Cluster of Differentiation 163 (CD163) and CD206) in THP-1 cells treated with CM. (H) RT-qPCR analysis of M2 markers in CM-treated THP-1 cells. (I) Schematic illustration of tumor-associated macrophage (TAM) induction by Phorbol 12-myristate 13-acetate (PMA)-differentiated M0 macrophages co-cultured with TPC-1 cells. (J,K) Flow cytometry was performed to analyze the expression of the M2 markers (CD163 and CD206) after co-culturing with TPC-1 cells. (L) RT-qPCR analysis of M2 markers in TAMs. (M) ALOX5 protein levels in macrophage subsets (M0, M2, TAM) were determined using Western blot analysis. Representative Western blot images are shown. (N) Quantification of ALOX5 protein expression levels from three independent experiments. (O) RT-qPCR analysis of *ALOX5* mRNA levels. All experiments were independently repeated at least three times. Data are presented as the mean ± SD. Statistical significance for all panels was assessed using one-way ANOVA. ns $p > 0.05$, ***$p < 0.001$.

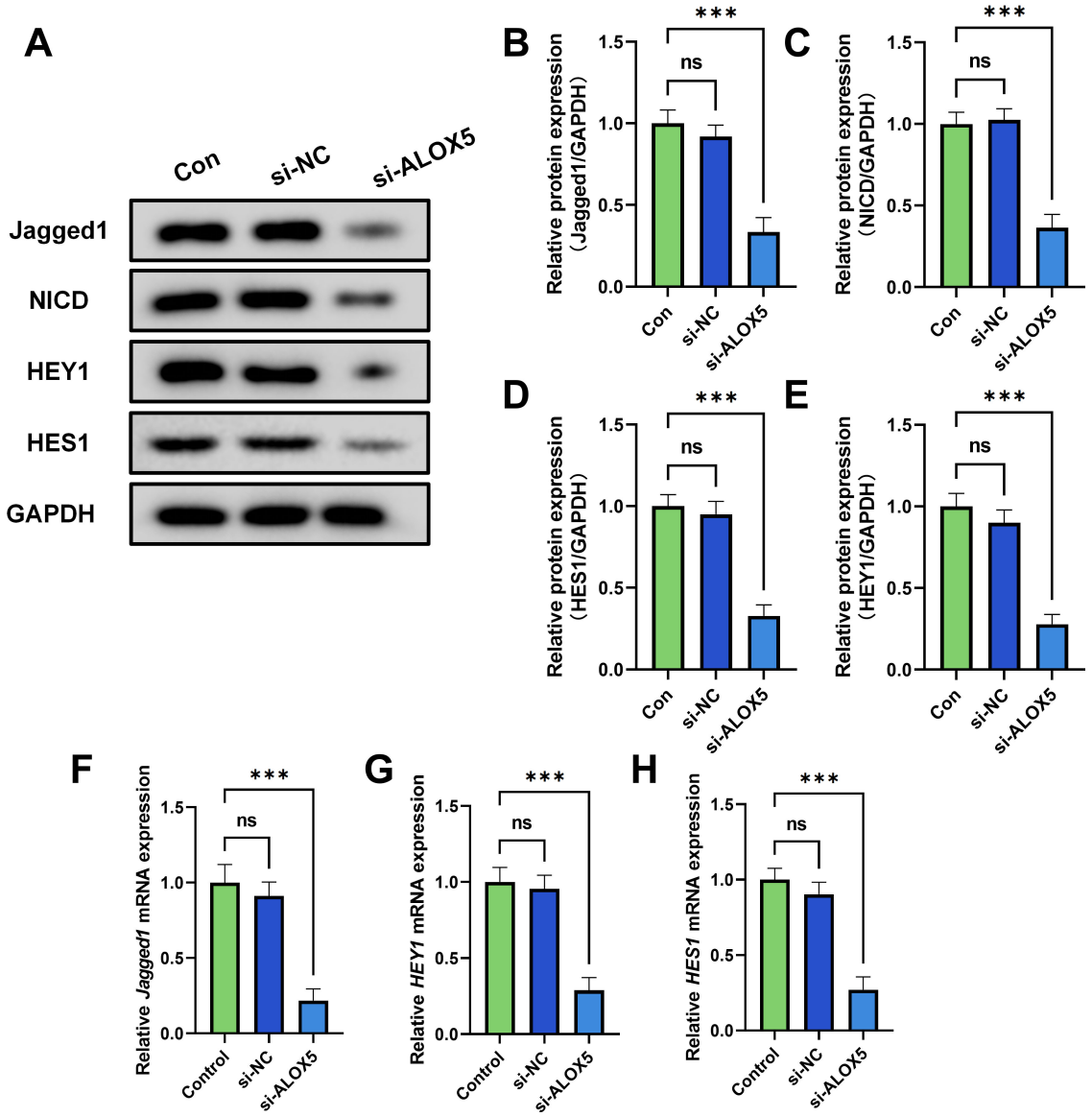

Fig. 5. Knockdown of ALOX5 attenuates the Notch signaling pathway in thyroid cancer cells. (A) Western blot analysis of Jagged1, NICD, Hairy/enhancer-of-split related with YRPW motif protein 1 (HEY1), and Hairy and enhancer of split-1 (HES1) protein expression levels. (B–E) Quantification of Jagged1, NICD, HES1, and HEY1 protein levels from three independent experiments. (F–H) RT-qPCR analysis of Jagged1, HEY1, and HES1 mRNA expression levels. All experiments were independently repeated at least three times. Data are presented as the mean ± SD. Statistical significance for all panels was assessed using one-way ANOVA. ns $p > 0.05$, ***$p < 0.001$.

These findings were further confirmed using a co-culture system, in which PMA-differentiated M0 macrophages were co-cultured with TPC-1 cells to induce TAM-like phenotypes. Consistent with the CM model, both flow cytometry and RT-qPCR analysis showed that ALOX5 knockdown in TPC-1 cells significantly alleviated the expression of CD163 and CD206 in co-cultured macrophages (Fig. 4I–L, $p < 0.001$), indicating a suppression of TAM polarization. Additionally, we assessed the endogenous ALOX5 expression in different macrophage subsets. Western blot and RT-qPCR analyses revealed significantly higher ALOX5 levels in M2 macrophages and TAMs compared with M0 macrophages (Fig. 4M–O, $p < 0.001$), suggesting a potential role of ALOX5 in maintaining or reinforcing the M2/TAM phenotype.

ALOX5 Silencing Inhibits the Jagged1-Notch Signaling in Thyroid Cancer Cells

To explore the downstream pathways regulated by ALOX5, we examined the Notch signaling cascade, which is known for its involvement in tumor progression and immune modulation. ALOX5 knockdown in TPC-1 cells resulted in a significant reduction in protein levels of Jagged1, NICD, HEY1, and HES1 (Fig. 5A–E, $p < 0.001$). Consis-

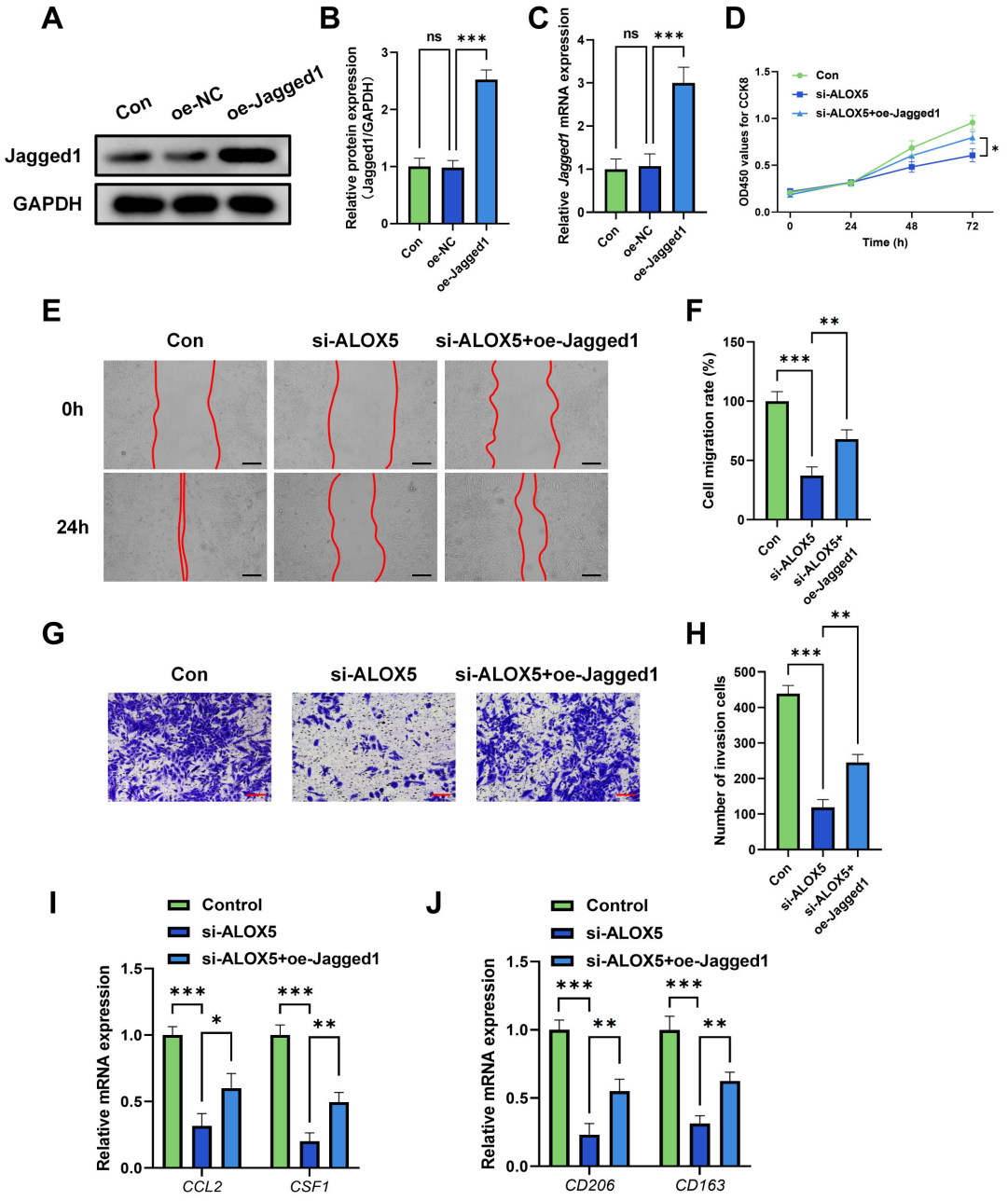

Fig. 6. Overexpression of Jagged1 reverses the inhibitory effects of ALOX5 knockdown on thyroid cancer cell progression and macrophage M2 polarization. (A) Western blot analysis of Jagged1 protein expression in the control, oe-NC, and oe-Jagged1 groups, representative images of three independent experiments. (B) Quantification of Jagged1 protein expression. (C) RT-qPCR analysis of *Jagged1* mRNA expression. (D) Cell proliferation assay of TPC-1 cells in the control, si-ALOX5, and si-ALOX5 + oe-Jagged1 groups. (E) Wound healing assay assessing the migration ability of TPC-1 cells (Scale bar: 100 μm). (F) Quantification of cell migration rate. (G) Transwell invasion assay evaluating the invasive ability of TPC-1 cells (Scale bar: 100 μm). (H) Quantification of the number of invading cells. (I) RT-qPCR analysis of *CCL2* and *CSF1* mRNA expression in the three groups. (J) RT-qPCR analysis of M2 macrophage markers *CD206* and *CD163* mRNA expression in the three groups. All experiments were independently repeated at least three times. Data are presented as the mean ± SD. Statistical significance for all panels was assessed using one-way ANOVA. ns $p > 0.05$, *$p < 0.05$, **$p < 0.01$, ***$p < 0.001$.

tently, RT-qPCR analysis showed a substantial downregulation of Jagged1, HEY1, and HES1 mRNA levels in the si-ALOX5 group (Fig. 5F–H, $p < 0.001$). These findings suggest that ALOX5 acts as a positive regulator of the Notch signaling pathway activity in thyroid cancer cells.

Jagged1 Overexpression Reverses the Suppressive Effects of ALOX5 Knockdown

To further validate the role of the Jagged1-Notch axis in ALOX5-mediated tumor progression, rescue experiments were performed by overexpressing Jagged1 in si-ALOX5–transfected TPC-1 cells. Western blot and RT-qPCR analyses confirmed the successful overexpression of Jagged1 (Fig. 6A–C, $p < 0.001$). Functional assays revealed that reintroducing Jagged1 reinstated the cell proliferation, migration, and invasion capacities that had been suppressed by ALOX5 knockdown (Fig. 6D–H, $p < 0.05$). Moreover, Jagged1 overexpression reversed the downregulation of CCL2, CSF1, and M2 markers (CD206, CD163) in si-ALOX5 cells (Fig. 6I,J, $p < 0.05$). Collectively, these results suggest that ALOX5 promotes thyroid cancer progression and immunosuppressive macrophage polarization via activation of the Jagged1-Notch signaling pathway.

Discussion

The global incidence of thyroid cancer has been increasing steadily, highlighting the urgent need for novel molecular targets to improve diagnosis and therapeutic approaches [23]. Although various oncogenic pathways are known to promote thyroid tumorigenesis, the role of lipid metabolic process-related enzymes, including ALOX5, in disease progression and modulation of the tumor-associated immune microenvironment remains poorly explained. In this study, we report novel evidence indicating that ALOX5 expression is significantly upregulated in both thyroid tumor tissues and cultured cancer cells, where it plays a pivotal role in enhancing malignant behaviors such as cellular proliferation, motility, and invasive capacity.

Consistent with previous studies associating ALOX5 with tumor growth and inflammation in other malignancies, such as pancreatic cancer and glioma [24,25], our findings extend its oncogenic potential to thyroid cancer. The significant inhibition of thyroid cancer cell growth and motility after ALOX5 silencing highlights its essential role in maintaining aggressive cancer phenotypes. These results suggest that ALOX5 could serve as a potential therapeutic target for managing thyroid cancer.

Moreover, this study identifies the immunomodulatory role of ALOX5, providing novel insights into its impact on the tumor microenvironment (TME). We found that ALOX5 positively regulates the expression of key macrophage chemoattractants and polarization-associated cytokines, CCL2 and CSF1, which are well-known to recruit macrophages and drive their polarization towards the tumor-promoting M2 phenotype. Conditioned media from ALOX5-deficient thyroid cancer cells failed to induce M2 macrophage markers CD163 and CD206, indicating that ALOX5 facilitates the formation of TAMs with an immunosuppressive and pro-tumorigenic phenotype. Notably, ALOX5 was found to be increased in both M2 macrophages and TAMs, suggesting the presence of a positive feedback loop that helps sustain an immunosuppressive TME.

Mechanistically, this study uncovered the Jagged1-Notch signaling pathway as a critical downstream mediator of ALOX5 function. Extensive evidence indicates Notch signaling as a modulator of cancer progression and immune regulation, including macrophage polarization [26]. We found that ALOX5 knockdown significantly downregulated Jagged1 and its downstream effectors, such as NICD, HEY1, and HES1, indicating suppression of canonical Notch signaling pathway activity. Importantly, overexpression of Jagged1 counteracted the suppressive impact of ALOX5 knockdown on tumor cell growth, motility, invasiveness, pro-inflammatory cytokine secretion, and the induction of M2-type macrophages. These findings demonstrate that ALOX5 exerts its pro-tumorigenic and immunomodulatory effects predominantly via activation of the Jagged1-Notch axis.

This study provides a comprehensive understanding of how ALOX5 integrates tumor cell intrinsic and microenvironmental signals to promote thyroid cancer progression. It expands the current knowledge of ALOX5 beyond its traditional role in lipid metabolism and inflammatory diseases, identifying it as a key modulator of immune-tumor crosstalk in thyroid cancer. Given the crucial role of TAMs in promoting disease progression and drug resistance, targeting the ALOX5-Jagged1-Notch signaling axis may offer a promising therapeutic strategy to inhibit tumor growth while reducing the associated immunosuppressive tumor microenvironment.

Despite significant outcomes, we acknowledge several limitations of this study. First, this study primarily investigated the impact of silencing ALOX5 to assess its role in thyroid cancer progression via the Jagged1-Notch pathway, further validation using ALOX5 overexpression combined with pharmacological inhibition of Notch (e.g., DAPT) could provide more comprehensive insights. Second, as ALOX5 is a multifunctional enzyme, it may promote tumor progression through pathways independent of Notch signaling, which were not explored in this study. Third, this study relied on TPC-1 cell lines to model the thyroid cancer immune microenvironment, which may not fully recapitulate the complexity of clinical tumor-immune interactions. Fourth, the lack of *in vivo* experiments and the limited access to clinical samples restrict the generalizability and translational strength of our findings. Hence, future studies incorporating non-Notch pathways, *in vivo* models, and clinical validation are warranted to improve the mechanistic and translational relevance of this work.

Conclusion

This study identifies ALOX5 as a novel oncogenic driver in thyroid cancer, promoting tumor progression and

immunosuppressive macrophage polarization through the Jagged1-Notch pathway. Targeting ALOX5 may represent a dual therapeutic approach, simultaneously suppressing tumor growth and remodeling the tumor immune microenvironment. Furthermore, given the crucial role of ALOX5 in the tumor immune landscape, future studies should investigate the therapeutic potential of combining ALOX5 inhibitors with immune checkpoint therapies, such as PD-1/PD-L1 antibodies, in thyroid cancer and potentially in other tumor types.

Availability of Data and Materials

The datasets used and/or analyzed during the current study are available from the corresponding author upon reasonable request.

Author Contributions

SL: Conceptualization, Methodology, Investigation, Data Curation, Formal Analysis, Writing – Original Draft. XL: Supervision, Project Administration, Resources, Data Processing, Figure Preparation, Validation, Writing – Critical revision of the manuscript. Both authors have read and approved the final manuscript. Both authors have participated sufficiently in the work and agreed to be accountable for all aspects of the work.

Ethics Approval and Consent to Participate

Not applicable.

Acknowledgment

Not applicable.

Funding

This research received no external funding.

Conflict of Interest

The authors declare no conflict of interest.

Supplementary Material

Supplementary material associated with this article can be found, in the online version, at https://doi.org/10.24976/Discov.Med.202537201.191.

References

[1] Boucai L, Zafereo M, Cabanillas ME. Thyroid Cancer: A Review. JAMA. 2024; 331: 425–435. https://doi.org/10.1001/jama.2023.26348.

[2] Zhang J, Xu S. High aggressiveness of papillary thyroid cancer: from clinical evidence to regulatory cellular networks. Cell Death Discovery. 2024; 10: 378. https://doi.org/10.1038/s41420-024-02157-2.

[3] Cai Y, Zhao L, Zhang Y, Luo D. Association between blood inflammatory indicators and prognosis of papillary thyroid carcinoma: a narrative review. Gland Surgery. 2024; 13: 1088–1096. https://doi.org/10.21037/gs-24-72.

[4] Jayawardana SAS, Samarasekera JKRR, Hettiarachchi GHCM, Gooneratne MJ. The pathogenetic roles of arachidonate 5-lipoxygenase, xanthine oxidase and hyaluronidase in inflammatory diseases: A review. Journal of Biomed Research. 2025; 6: 26–31.

[5] Luo Y, Jin M, Lou L, Yang S, Li C, Li X, *et al*. Role of arachidonic acid lipoxygenase pathway in Asthma. Prostaglandins & other Lipid Mediators. 2022; 158: 106609. https://doi.org/10.1016/j.prostaglandins.2021.106609.

[6] Li M, Xin S, Gu R, Zheng L, Hu J, Zhang R, *et al*. Novel Diagnostic Biomarkers Related to Oxidative Stress and Macrophage Ferroptosis in Atherosclerosis. Oxidative Medicine and Cellular Longevity. 2022; 2022: 8917947. https://doi.org/10.1155/2022/8917947.

[7] Ji Z, Li X, Gao W, Xia Q, Li J. ALOX5 induces EMT and promotes cell metastasis via the LTB4/BLT2/PI3K/AKT pathway in ovarian cancer. Cellular Signalling. 2024; 124: 111404. https://doi.org/10.1016/j.cellsig.2024.111404.

[8] Chi B, Sun Y, Zhao J, Guo Y. Deoxyschizandrin Inhibits the Proliferation, Migration, and Invasion of Bladder Cancer Cells through ALOX5 Regulating PI3K-AKT Signaling Pathway. Journal of Immunology Research. 2022; 2022: 3079823. https://doi.org/10.1155/2022/3079823.

[9] Tang J, Zhang C, Lin J, Duan P, Long J, Zhu H. ALOX5-5-HETE promotes gastric cancer growth and alleviates chemotherapy toxicity via MEK/ERK activation. Cancer Medicine. 2021; 10: 5246–5255. https://doi.org/10.1002/cam4.4066.

[10] Zhao Q, Sun Z, Pan Y, Jing Q, Li W, Wang C. Role of ALOX5 in non-small cell lung cancer: A potential therapeutic target associated with immune cell infiltration. Zhong Nan Da Xue Xue Bao. Yi Xue Ban = Journal of Central South University. Medical Sciences. 2023; 48: 311–322. https://doi.org/10.11817/j.issn.1672-7347.2023.220427.

[11] Hu WM, Liu SQ, Zhu KF, Li W, Yang ZJ, Yang Q, *et al*. The ALOX5 inhibitor Zileuton regulates tumor-associated macrophage M2 polarization by JAK/STAT and inhibits pancreatic cancer invasion and metastasis. International Immunopharmacology. 2023; 121: 110505. https://doi.org/10.1016/j.intimp.2023.110505.

[12] Zou W, Green DR. Beggars banquet: Metabolism in the tumor immune microenvironment and cancer therapy. Cell Metabolism. 2023; 35: 1101–1113. https://doi.org/10.1016/j.cmet.2023.06.003.

[13] Xiang X, Wang J, Lu D, Xu X. Targeting tumor-associated macrophages to synergize tumor immunotherapy. Signal Transduction and Targeted Therapy. 2021; 6: 75. https://doi.org/10.1038/s41392-021-00484-9.

[14] Qian Y, Yin Y, Zheng X, Liu Z, Wang X. Metabolic regulation of tumor-associated macrophage heterogeneity: insights into the tumor microenvironment and immunotherapeutic opportunities. Biomarker Research. 2024; 12: 1. https://doi.org/10.1186/s40364-023-00549-7.

[15] Huang R, Kang T, Chen S. The role of tumor-associated macrophages in tumor immune evasion. Journal of Cancer Research and Clinical Oncology. 2024; 150: 238. https://doi.org/10.1007/s00432-024-05777-4.

[16] Patysheva M, Frolova A, Larionova I, Afanas'ev S, Tarasova A, Cherdyntseva N, *et al*. Monocyte programming by cancer therapy. Frontiers in Immunology. 2022; 13: 994319. https://doi.org/10.3389/fimmu.2022.994319.

[17] Zhou B, Lin W, Long Y, Yang Y, Zhang H, Wu K, *et al*. Notch signaling pathway: architecture, disease, and therapeu-

tics. Signal Transduction and Targeted Therapy. 2022; 7: 95. https://doi.org/10.1038/s41392-022-00934-y.

[18] Mukerjee N, Nag S, Bhattacharya B, Alexiou A, Mirgh D, Mukherjee D, *et al*. Clinical impact of epithelial–mesenchymal transition for cancer therapy. Clinical and Translational Discovery. 2024; 4: e260.

[19] D'Assoro AB, Leon-Ferre R, Braune EB, Lendahl U. Roles of Notch Signaling in the Tumor Microenvironment. International Journal of Molecular Sciences. 2022; 23: 6241. https://doi.org/10.3390/ijms23116241.

[20] Wang C, Ma C, Gong L, Guo Y, Fu K, Zhang Y, *et al*. Macrophage Polarization and Its Role in Liver Disease. Frontiers in Immunology. 2021; 12: 803037. https://doi.org/10.3389/fimmu.2021.803037.

[21] Liu L, Zhao WY, Zheng XY. ZNF746 promotes M2 macrophage polarisation and favours tumour progression in breast cancer via the Jagged1/Notch pathway. Cellular Signalling. 2023; 112: 110892. https://doi.org/10.1016/j.cellsig.2023.110892.

[22] Ren L, Yi J, Yang Y, Li W, Zheng X, Liu J, *et al*. Systematic pan-cancer analysis identifies APOC1 as an immunological biomarker which regulates macrophage polarization and promotes tumor metastasis. Pharmacological Research. 2022; 183: 106376. https://doi.org/10.1016/j.phrs.2022.106376.

[23] Miranda-Filho A, Lortet-Tieulent J, Bray F, Cao B, Franceschi S, Vaccarella S, *et al*. Thyroid cancer incidence trends by histology in 25 countries: a population-based study. The Lancet. Diabetes & Endocrinology. 2021; 9: 225–234. https://doi.org/10.1016/S2213-8587(21)00027-9.

[24] Chen T, Liu J, Wang C, Wang Z, Zhou J, Lin J, *et al*. ALOX5 contributes to glioma progression by promoting 5-HETE-mediated immunosuppressive M2 polarization and PD-L1 expression of glioma-associated microglia/macrophages. Journal for Immunotherapy of Cancer. 2024; 12: e009492. https://doi.org/10.1136/jitc-2024-009492.

[25] Wu L, Liang F, Chen C, Zhang Y, Huang H, Pan Y. Identification of prognostic and therapeutic biomarkers associated with macrophage and lipid metabolism in pancreatic cancer. Scientific Reports. 2025; 15: 14584. https://doi.org/10.1038/s41598-025-99144-z.

[26] Chen X, Wang F, Tang J, Meng J, Han Z. Paralemmin-3 augments lipopolysaccharide-induced acute lung injury with M1 macrophage polarization via the notch signaling pathway. Respiratory Physiology & Neurobiology. 2024; 320: 104203. https://doi.org/10.1016/j.resp.2023.104203.